

# Singularities in the acoustic Casimir pressure as a function of reflectivities

T. J. Liebau

*Department of Biomedical Engineering and Mechanics, Virginia Tech, Blacksburg, VA 24060, USA.*

*Ronin Institute, 127 Haddon Place, Montclair, NJ 07043, USA.*

June 22, 2021

**Abstract.** We study the acoustic Casimir pressure between imperfectly reflecting plates immersed in various isotropic noise backgrounds. For flat as well as narrowly peaked noise spectra, the force tends to strong repulsion as the plate separation tends to zero, in contrast to the case of perfect reflectors. We uncover and analyze the associated singular behavior as the product of the reflection coefficients approaches 1, obtaining in the process expressions for the pressure resulting from arbitrary power-law spectra.

## Introduction

Two parallel plates in a random acoustic field will experience a force analogous to the quantum Casimir force [1]. Owing to the finite bandwidth of the noise, this force can be either attractive or repulsive depending on the plate separation. Larraza et al. [2] proposed and experimentally demonstrated this acoustic Casimir effect, while also providing the theory for perfectly reflecting plates.

If the plates are not perfectly reflective, the wavevector component perpendicular to the plates is no longer restricted to integer multiples of  $\pi/L$ , and the total density of modes must be calculated. Esquivel-Sirvent et al. [3] derived an expression for the resulting pressure using a Green's function approach. In this work, we apply their expression to uncover a subtle behavior of the acoustic Casimir force at small plate separations, which does not occur for perfect reflectors.

When perfectly reflecting plates are separated by less than the smallest half-wavelength contained in the background noise, the force is attractive and independent of the separation (no modes exist between the plates) [2]. This is no longer the case for imperfect reflectors, and when the noise intensity is constant over the considered bandwidth, there is actually a small value of the plate separation below which the force rapidly tends to repulsion. This can be viewed as a critical phenomenon, and we derive an associated quantity  $\tilde{q}_c \sim (1 - \eta)^{1/2}$  as  $\eta \rightarrow 1$ ; the quantity  $\tilde{q}_c$  is a dimensionless critical plate separation or infrared wavenumber cutoff depending on the context, and  $\eta$  is the product of the reflectivities of the plates.

We then turn to power-law noise spectra, paying close attention to infinite-bandwidth limits; and finally to narrow unimodal spectra, inspired by the formalism of Lee et al. [4]. The case of imperfect reflectors in a narrowly peaked noise background exhibits singular behavior analogous to that described above.

## Flat spectra and critical phenomena

Consider two parallel rigid plates with reflectivities  $r_A, r_B$  separated by a distance  $L$ , and define  $\eta \equiv r_A r_B$ . If the plates are immersed in an isotropic noise field of constant spectral intensity  $I_\omega$  within the frequency range  $[f_1, f_2]$ , the resulting net pressure is  $\text{Re}[P]$ , where [3]

$$P(\eta, L, q_1, q_2) = \frac{I_\omega}{2\pi} \iiint_{q_1 < |\mathbf{k}| < q_2} dk_x dk_y dk_z \frac{k_z^2}{|\mathbf{k}|^4} \frac{1}{\eta^{-1} e^{-2ik_z L} - 1} \quad (1)$$

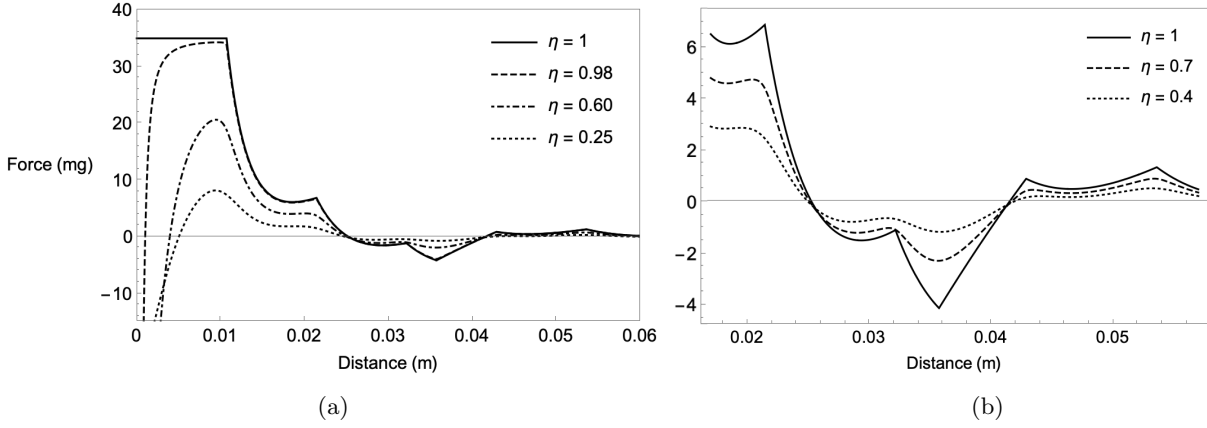


Figure 1: Band-limited acoustic Casimir force between imperfect reflectors. An attractive/repulsive force is given by a positive/negative value respectively. Here  $f_1 = 4.8$  kHz,  $f_2 = 16$  kHz,  $I_\omega = 2.84 \cdot 10^{-4}$  J/m<sup>2</sup>,  $c = 343$  m/s and the area of each plate is  $1.77 \cdot 10^{-2}$  m<sup>2</sup>.

and  $q_{1,2} = 2\pi f_{1,2}/c$ . If  $\eta$  is constant over the considered bandwidth, this integral can be expressed in terms of polylogarithms [5]: for  $|\eta| \leq 1$ ,

$$\begin{aligned}
P &= I_\omega \int_0^\pi d\phi \sin \phi \int_{q_1}^{q_2} dq \frac{\cos^2 \phi}{\eta^{-1} e^{-2iLq \cos \phi} - 1} \\
&= I_\omega \int_{-1}^1 du \int_{q_1}^{q_2} dq \frac{u^2}{\eta^{-1} e^{-2iuLq} - 1} \\
&= I_\omega \int_{-1}^1 du \frac{i u}{2L} [\ln(1 - \eta e^{2iuLq_2}) - \ln(1 - \eta e^{2iuLq_1})] \\
&= \frac{I_\omega}{L} [F(Lq_1) - F(Lq_2)]
\end{aligned} \tag{2}$$

where

$$F(\tilde{q}) \equiv F(\tilde{q}, \eta) = \frac{\text{Li}_2(\eta e^{-2i\tilde{q}})}{4\tilde{q}} + \frac{\text{Li}_2(\eta e^{2i\tilde{q}})}{4\tilde{q}} + \frac{\text{Li}_3(\eta e^{-2i\tilde{q}})}{8i\tilde{q}^2} - \frac{\text{Li}_3(\eta e^{2i\tilde{q}})}{8i\tilde{q}^2}, \tag{3}$$

and

$$\text{Li}_m(z) \equiv \sum_{n=1}^{\infty} \frac{z^n}{n^m}.$$

In Fig. 1, we plot  $-P(L)$  with fixed noise parameters for different values of  $\eta$ . As  $\eta \rightarrow 1$ , the result converges to that of Larraza et al. [2]. For sufficiently large plate separation, the main action of reduced reflectivity, besides reducing the magnitude of the force, is the smoothing of the kinks at which  $q_{1,2}L/\pi$  is an integer. In this example, the ranges of  $L$  in which the force is attractive/repulsive are barely affected by  $\eta$  for  $L > \pi/q_2$ . For  $L < \pi/q_2$ , the behavior differs remarkably from the  $\eta = 1$  case; the force is no longer constant in  $L$ , and actually becomes repulsive for small enough  $L$ : we have

$$\lim_{L \rightarrow 0} P(1, L, q_1, q_2) = I_\omega \cdot \frac{q_1 - q_2}{3},$$

but if  $\eta \neq 1$ ,

$$\lim_{L \rightarrow 0} P(\eta, L, q_1, q_2) = I_\omega \cdot \frac{2\eta}{3} \left( \frac{q_1 - q_2}{\eta - 1} \right), \tag{4}$$

which diverges as  $\eta \rightarrow 1$ .

This can be resolved in part by investigating the small- $\tilde{q}$  behavior of  $F(\tilde{q}, \eta)$  as  $\eta \rightarrow 1$ . First note that  $F \rightarrow 0$  as  $\tilde{q} \rightarrow \infty$ . For  $\eta = 1$ , we see that  $F$  tends to  $-\pi/4$  as  $\tilde{q} \rightarrow 0$ , as expected since in the infinite-bandwidth limit for perfect reflectors [2],  $P = -\pi I_\omega/4L$ . However, if  $\eta \neq 1$  then the  $\tilde{q} \rightarrow 0$  limit is actually zero. For  $\eta$  slightly less than 1,  $F$  has a minimum at some small  $\tilde{q}_c$ , with  $F(\tilde{q}_c)$  slightly greater than  $-\pi/4$ . As  $\tilde{q}$  is varied from  $\tilde{q}_c$  to 0,  $F$  rapidly rises to zero (cf. Fig. 2).

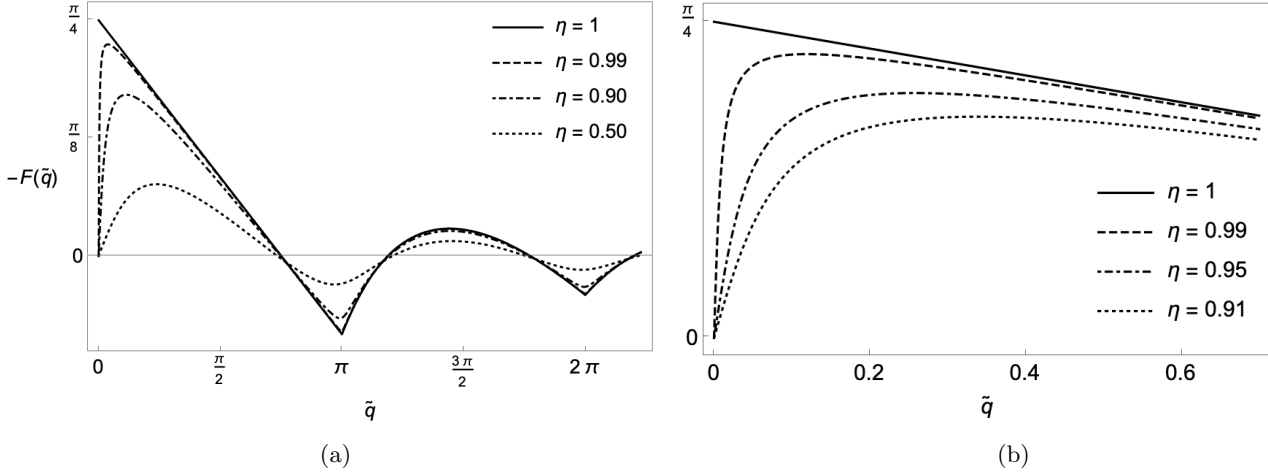


Figure 2: The singular behaviour of  $F(\tilde{q}, \eta)$  as  $\eta$  approaches 1.

We consider  $\tilde{q}_c(\eta)$  as a nondimensional cutoff, and study its behavior as  $\eta \rightarrow 1$ . To this end, we define

$$\psi(\tau, \tilde{q}) \equiv \left. \frac{\partial F}{\partial \tilde{q}} \right|_{\eta \rightarrow 1 - \tau} \quad \psi_0(\tilde{q}) \equiv \psi(0, \tilde{q}) \quad \psi_1(\tilde{q}) \equiv - \left. \frac{\partial \psi}{\partial \tau} \right|_{(0, \tilde{q})}$$

where  $\tau \equiv 1 - \eta > 0$  plays a role analogous to a reduced temperature, and now

$$\tilde{q}_c = \min\{\tilde{q} \mid \psi(\tau, \tilde{q}) = 0 \ \& \ \tilde{q} > 0\}.$$

As  $\tau \rightarrow 0$ , we have to lowest order in  $\tilde{q}_c$ ,

$$\psi(\tau, \tilde{q}_c) = \psi_0(\tilde{q}_c) - \tau \psi_1(\tilde{q}_c) = 0 \implies \tau = \frac{\psi_0(\tilde{q}_c)}{\psi_1(\tilde{q}_c)} = \frac{2\tilde{q}_c^2}{3} \Leftrightarrow \boxed{\tilde{q}_c(\eta) = \sqrt{\frac{3}{2}}(1 - \eta)^{1/2}} \quad (5)$$

and

$$F(\tilde{q}_c, 1 - \frac{2}{3}\tilde{q}_c^2) = \frac{2\tilde{q}_c}{3} - \frac{\pi}{4} \Leftrightarrow \boxed{F(\tilde{q}_c(\eta), \eta) = \sqrt{\frac{2}{3}}(1 - \eta)^{1/2} - \frac{\pi}{4}} \quad (6)$$

This analysis is confirmed by numerically solving for the first zero of  $\psi(\tau, \tilde{q})$  without taking any expansion. We find that over the range  $0.9 < \eta < 1$ , the relations

$$\tau = \frac{2\tilde{q}_c^2}{3} + 0.349\tilde{q}_c^3 \quad (7)$$

and

$$F(\tilde{q}_c, 1 - \frac{2}{3}\tilde{q}_c^2 - 0.349\tilde{q}_c^3) = \frac{2\tilde{q}_c}{3} + 0.0872\tilde{q}_c^2 - \frac{\pi}{4} \quad (8)$$

are accurate to less than 1% relative error.

If we are interested in well-posed large-bandwidth limits, we can impose an infrared cutoff  $q_c = \tilde{q}_c(\eta)/L_0$  on the noise field and define  $L_0$  as the minimum length under consideration; then

$$\lim_{q_2 \rightarrow \infty} P\left(\eta, L, \frac{\tilde{q}_c(\eta)}{L_0}, q_2\right) \equiv P^{(q_c, \infty)}(\eta, L, L_0) = \frac{I_\omega}{L} F\left(\tilde{q}_c(\eta) \frac{L}{L_0}, \eta\right), \quad L \geq L_0$$

with  $F$  given by Eq. (3). If  $\eta$  is near 1, then  $P^{(q_c, \infty)}(\eta, L_0, L_0)$  is slightly greater than  $-\pi I_\omega/4L_0$ , cf. Fig. 3b. Furthermore, since  $\tilde{q}_c$  is small,  $P^{(q_c, \infty)} \approx -\pi I_\omega/4L$  over a considerable range of  $L/L_0$ , up to the point where  $F\left(\tilde{q}_c(\eta) \frac{L}{L_0}\right)$  becomes too small; perhaps around  $\tilde{q}_c L/L_0 = \pi/4$ , cf. Fig 2a. At around  $\tilde{q}_c L/L_0 = 3\pi/4$ , the force becomes repulsive, and slowly oscillates between attractive and repulsive as  $L/L_0$  increases further.

If the wavenumber band  $[q_1, q_2]$  is fixed, we can consider  $L_c = \tilde{q}_c(\eta)/q_1$  as a critical plate separation, at which the force is attractive and below which the the force rapidly tends to repulsion. In the example of Fig. 1, for  $\eta = 0.98$ , we have  $L_c \approx 2$  mm and a corresponding force of about 25 mg.

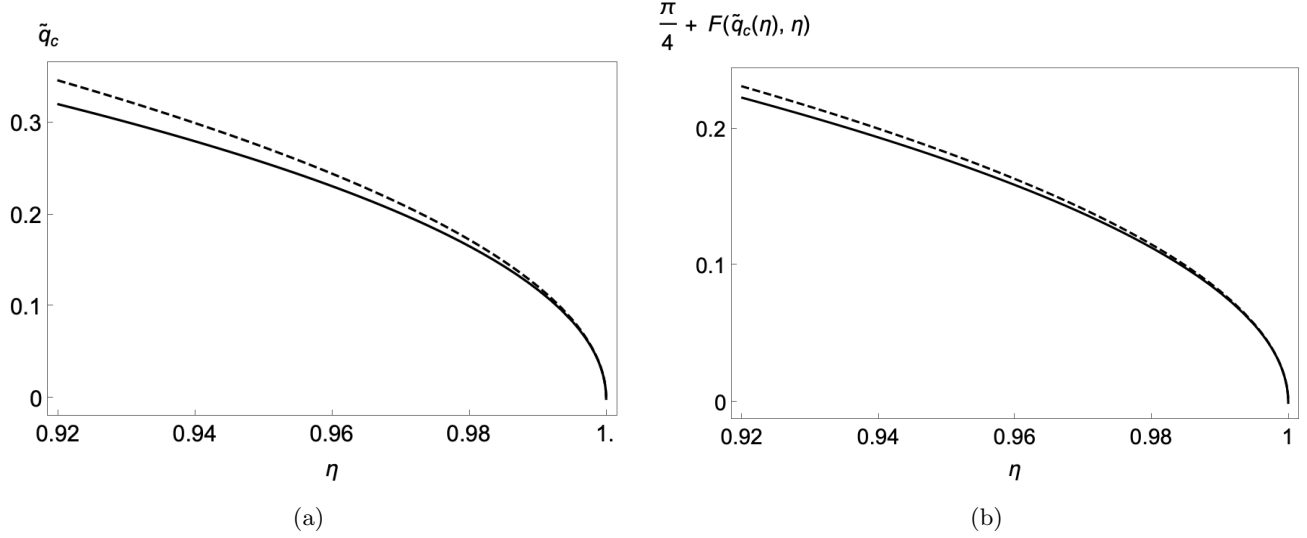


Figure 3: (a) The cutoff, and (b) corresponding difference between  $F$  and  $-\pi/4$  as  $\eta \rightarrow 1$ . The solid lines are given by Eqs. (7) and (8) and are visually indistinguishable from numerical solutions. The dashed lines are given by Eqs. (5) and (6).

## Power-law and narrow unimodal spectra

Next, we consider energy spectra well described by  $G(q) \propto q^\alpha$  over a particular wavenumber range. The corresponding Casimir pressure is proportional to  $\text{Re}[P_\alpha]$ , where

$$P_\alpha(\eta, L, q_1, q_2) = \int_{q_1}^{q_2} dq q^\alpha \int_{-1}^1 du \frac{u^2}{\eta^{-1} e^{-2iuLq} - 1}. \quad (9)$$

Carrying out the  $u$ -integration first,

$$\int_{-1}^1 du \frac{u^2}{\eta^{-1} e^{-2iuLq} - 1} = f(Lq) + f(-Lq),$$

where

$$f(\tilde{q}) = \frac{\ln(1 - \eta e^{-2i\tilde{q}})}{2i\tilde{q}} + \frac{\text{Li}_2(\eta e^{-2i\tilde{q}})}{2\tilde{q}^2} + \frac{\text{Li}_3(\eta e^{-2i\tilde{q}})}{4i\tilde{q}^3}. \quad (10)$$

Since  $|\eta| \leq 1$ , we can express this in series form and carry out the  $q$ -integration term-by-term. The result is

$$\begin{aligned} P_\alpha(\eta, L, q_1, q_2) &= \sum_{n=1}^{\infty} \eta^n \int_{q_1}^{q_2} dq \left[ e^{-2inLq} \left( \frac{q^{\alpha-3}}{4in^3L^3} + \frac{q^{\alpha-2}}{2n^2L^2} - \frac{q^{\alpha-1}}{2inL} \right) + \text{c.c.} \right] \\ &= \frac{1}{L^{1+\alpha}} \sum_{n=1}^{\infty} \eta^n [f_{n,\alpha}(Lq_1) - f_{n,\alpha}(Lq_2)], \end{aligned} \quad (11)$$

where

$$f_{n,\alpha}(\tilde{q}) = \frac{\tilde{q}^{\alpha-2}}{4in^3} E_{3-\alpha}(2in\tilde{q}) + \frac{\tilde{q}^{\alpha-1}}{2n^2} E_{2-\alpha}(2in\tilde{q}) - \frac{\tilde{q}^\alpha}{2in} E_{1-\alpha}(2in\tilde{q}) + \text{c.c.} \quad (12)$$

and

$$E_m(z) \equiv \int_1^\infty dt \frac{e^{-zt}}{t^m}.$$

This result, like the flat-spectrum case, is a simple function of  $L$  times a more complicated function of  $\tilde{q}_{1,2} \equiv Lq_{1,2}$ . In Fig. 4a we display

$$F_\alpha(\tilde{q}, \eta) \equiv \sum_{n=1}^{\infty} \eta^n f_{n,\alpha}(\tilde{q})$$

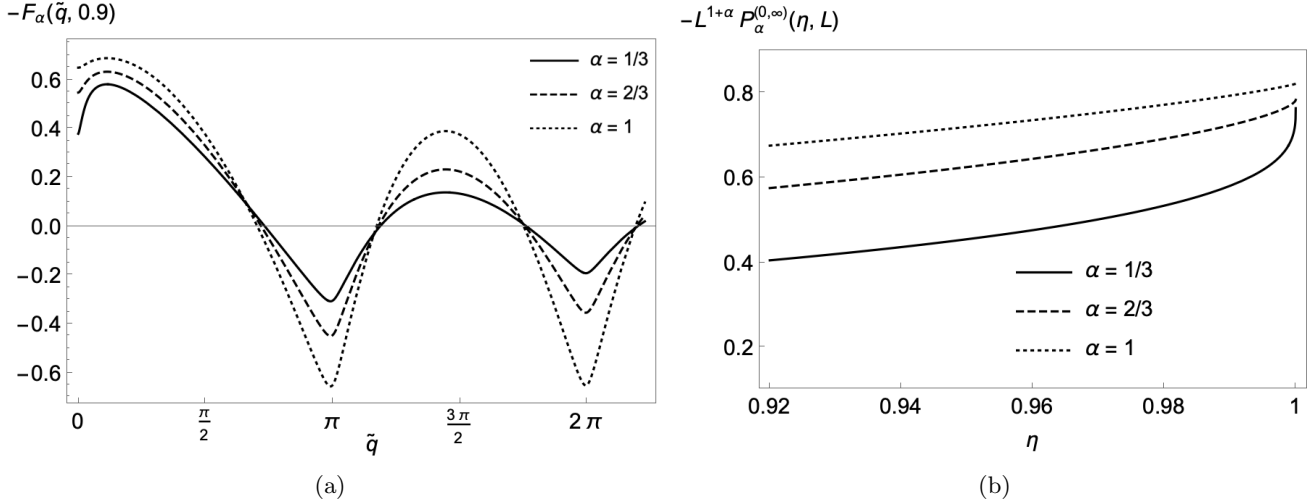


Figure 4: Analysis of power-law spectra,  $G(q) \propto q^\alpha$ . (a)  $F_\alpha$  vs.  $\tilde{q}$  for  $\eta = 0.9$ . The variation at small  $\tilde{q}$  is sharper for lower  $\alpha$ . As  $\tilde{q} \rightarrow \infty$ ,  $F_{1/3}$  decays faster than does  $F_{2/3}$ , and the oscillations of  $F_1$  neither decay nor grow. (b) Infinite-bandwidth limits as a function of  $\eta$  for various  $\alpha$ . The case  $\alpha = 1/3$  displays relatively sharp variation as  $\eta$  approaches 1.

for various  $\alpha$  with  $\eta = 0.9$ .

The functions  $E_m(z)$  each have a branch cut running along the negative real axis, and the small- $q$  limit of  $F_\alpha(Lq)$  is determined by the behavior as the branch points at zero are approached along both sides of the imaginary axis. We have

$$\frac{f_{n,\alpha}(Lq)}{L^{1+\alpha}} \rightarrow \frac{1}{n^{1+\alpha}} \frac{2^{-\alpha}}{L^{1+\alpha}} \frac{\Gamma(1+\alpha)}{\alpha-2} \sin\left(\frac{\alpha\pi}{2}\right) - \frac{2q^{\alpha+1}}{3(\alpha+1)} \quad \text{as } q \rightarrow 0^+$$

where  $\Gamma$  is the gamma function. This converges for  $\alpha > -1$ , while the large- $q$  limit,

$$\frac{f_{n,\alpha}(Lq)}{L^{1+\alpha}} \rightarrow \frac{q^{\alpha-1}}{n^2 L^2} \cos(2nLq) \quad \text{as } q \rightarrow \infty$$

is 0 for  $\alpha < 1$ . Thus an infinite-bandwidth limit exists for  $-1 < \alpha < 1$  and is given by

$$\lim_{q \rightarrow 0^+} \frac{F_\alpha(Lq)}{L^{1+\alpha}} \equiv P_\alpha^{(0,\infty)}(\eta, L) = -\frac{2^{-\alpha}}{L^{1+\alpha}} \frac{\Gamma(1+\alpha)}{2-\alpha} \sin\left(\frac{\alpha\pi}{2}\right) \text{Li}_{1+\alpha}(\eta), \quad (13)$$

which itself diverges as  $\alpha \rightarrow -1$ , and which for any  $\alpha < 0$  implies a repulsive force when  $\eta > 0$  and diverges in the limit of perfect reflectors  $\eta \rightarrow 1$ . This formula illustrates the sharp variation in  $\eta$ , as  $\eta$  approaches 1, of the  $q \rightarrow 0$  limit when  $\alpha$  is greater than, but close to zero. In particular, we have as  $\alpha \rightarrow 0^+$ ,

$$P_\alpha^{(0,\infty)}(1, L) \rightarrow -\frac{1}{2L} \lim_{\alpha \rightarrow 0^+} \left[ \sin\left(\frac{\alpha\pi}{2}\right) \text{Li}_{1+\alpha}(1) \right] = -\frac{\pi}{4L},$$

whereas for  $\eta < 1$ ,  $P_0^{(0,\infty)}(\eta, L)$  is strictly zero as expected. The  $L$ -independent part of  $P_\alpha^{(0,\infty)}$  is displayed in Fig. 4b. We can also get the marginal  $\alpha \rightarrow 1$  case,

$$P_1^{(0,\infty)}(\eta, L) = -\frac{\text{Li}_2(\eta)}{2L^2}$$

which is  $-\pi^2/12L^2$  for perfect reflectors.

Finally, we investigate narrow unimodal spectra where  $G(q)$  has a maximum at some  $q_0$ . First consider that if  $G(q) \propto \delta(q - q_0)$ , then

$$P_\delta(\eta, \tilde{L}) = f(\tilde{L}) + f(-\tilde{L}) = -\left. \frac{\partial F}{\partial \tilde{q}} \right|_{\tilde{q}=\tilde{L}} \quad (14)$$

where  $\tilde{L} \equiv q_0 L$ , with  $f$  defined by Eq. (10) and  $F$  defined by Eq. (3). Again, there is non-trivial behavior as  $\eta \rightarrow 1$  for small  $\tilde{L}$ : we have

$$\lim_{\tilde{L} \rightarrow 0} P_\delta(1, \tilde{L}) = -\frac{1}{3};$$

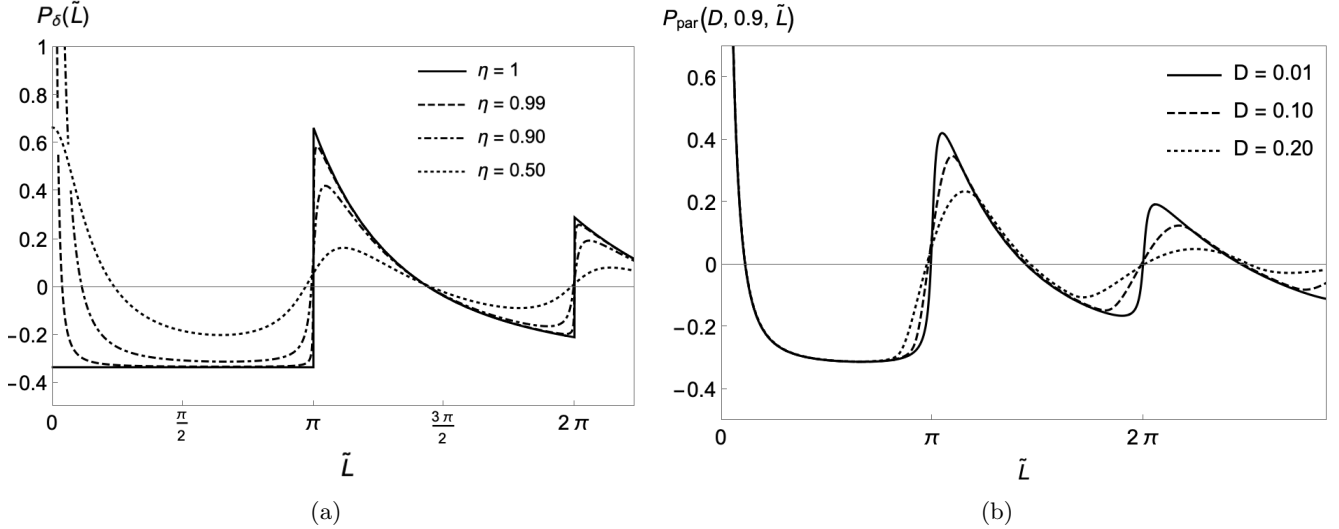


Figure 5: Casimir pressure resulting from narrowly peaked spectra. (a) Delta-function spectrum for various  $\eta$ . (b) Parabolic spectrum for various peak widths with  $\eta = 0.9$ . The prediction of rapid variation near  $\tilde{L} = \tilde{q}_c(\eta)$  is confirmed. When  $D = 0.01$ , the corresponding pressure is indistinguishable from  $P_\delta(0.9, \tilde{L})$  over this range, but this would not be the case for larger  $\tilde{L}$ .

$$\lim_{\tilde{L} \rightarrow 0} P_\delta(\eta, \tilde{L}) = \frac{2\eta}{3(1-\eta)}, \quad \eta \neq 1. \quad (15)$$

$P_\delta(\tilde{L})$  is plotted in Fig. 5a for different values of  $\eta$ . As  $\tilde{L}$  is increased past an integer multiple of  $\pi$ , the force rapidly switches from attractive to repulsive, becoming discontinuous in the limit of perfect reflectors. The cutoff  $\tilde{q}_c(\eta)$  from Eqs. (5) and (7) gives the lowest value of  $\tilde{L}$  at which  $P_\delta(\tilde{L})$  is zero; when  $\eta$  is near 1,  $P_\delta$  quickly falls to a value slightly greater than  $-1/3$  as  $\tilde{L}$  is increased from  $\tilde{q}_c$ . Below  $\tilde{q}_c$ , the force is repulsive, rapidly increasing in magnitude as  $\tilde{L}$  is decreased further. If one considers  $q_0$  fixed, then  $\tilde{q}_c$  is a dimensionless critical separation, i.e.  $L_c = \tilde{q}_c/q_0$ .

We would like to see if this phenomena holds for general narrowly peaked spectra. Taylor expanding an appropriate  $G(q)$  about its maximum at  $q_0$  gives a parabolic approximation [4],  $G(q) \propto G_{\text{par}}(q)$ , where

$$G_{\text{par}}(q) = \max \left\{ \frac{3}{4q_0 D} \left[ 1 - \left( \frac{q - q_0}{q_0 D} \right)^2 \right], 0 \right\}.$$

The dimensionless parameter  $D < 1$  relates to the width of the peak. This is equivalent to a weighted sum of three spectra, proportional to 1,  $q$ , and  $q^2$  respectively, over the finite band  $[q_0 - q_0 D, q_0 + q_0 D]$ . From Eq. (9), the resulting pressure is

$$P_{\text{par}}(D, \eta, \tilde{L}) = \frac{3}{D^3} \left[ \frac{D^2 - 1}{4q_0} P_0^{\{q_0, D\}}(\eta, L) + \frac{1}{2q_0^2} P_1^{\{q_0, D\}}(\eta, L) - \frac{1}{4q_0^3} P_2^{\{q_0, D\}}(\eta, L) \right], \quad (16)$$

where

$$P_\alpha^{\{q_0, D\}}(\eta, L) \equiv P_\alpha(\eta, L, q_0 - q_0 D, q_0 + q_0 D).$$

Note that  $\int_0^\infty dq G_{\text{par}}(q) = 1$ , and that the corresponding pressure depends on  $q_0 L$  and not separately on  $q_0$  or  $L$ , cf. Eq. (11).  $P_0$  is just  $P/L_\omega$  from Eqs. (2)-(3); a similar form of  $P_1$ , computationally more expedient than the result of (11)-(12), can be derived along the same lines of (2). For  $P_2$  this is not the case, but the form given by (11)-(12) is advantageous over numerical integration [6].

The result for  $\eta = 0.9$  is plotted in Fig. 5b for various  $D$ . The phenomena near  $\tilde{q}_c$  persists, and is in fact insensitive to the peak width! The effect of larger widths comes into play at larger  $\tilde{L}$ , involving the fact that  $n\pi(1-D)$  and  $n\pi(1+D)$ ,  $n$  an integer, become more spaced apart as  $n$  increases; the alternations between attraction and repulsion become less rapid, and this effect is more pronounced for larger  $D$ .

## Conclusions

We have derived expressions for the pressure between two imperfectly reflecting plates immersed in random acoustic fields. The asymptotic properties of the associated special functions reveal singular behavior as the product of the plate

reflectivities approaches unity, leaving a crucial imprint on the sign and magnitude of the force between closely-spaced plates in flat or nonmonotonic spectral backgrounds. The closer the plates are to perfect reflectors, the stronger the repulsion in the limit of no separation between the plates; while at the same time, increasingly small plate separations are required for attraction to cease. It would be interesting to extend the analysis to include plate deformations due to the noise field [3] and prescribed spatiotemporal modulations of the plates [5,7].

For completeness, we remark on the pressure between two plates with negative or complex  $\eta$ . If plate A is a perfect reflector,  $r_A = 1$ , and plate B is a pressure release surface,  $r_B = -1$ , then  $\eta = -1$  and the wavevector component perpendicular to the plates can only take on values  $(n\pi - \frac{\pi}{2})/L$ , where  $n$  is an integer. The kinks, when  $G(q) \propto q^\alpha$  over a finite band  $[q_1, q_2]$ , and discontinuities, when  $G(q) \propto \delta(q - q_0)$ , then occur at  $Lq_{0,1,2} = n\pi - \frac{\pi}{2}$  rather than  $n\pi$ .

If  $G(q) \propto 1$ , then the infinite-bandwidth limit is zero, in contrast to when  $\eta = 1$ , but the  $L \rightarrow 0$  limit under finite bandwidth is the same as that of  $\eta = 1$ . Furthermore, if  $G(q) \propto \delta(q - q_0)$ , then the  $L \rightarrow 0$  limit is  $-1/3$ , the same as when  $\eta$  is strictly 1. No singular behavior occurs as  $\eta$  is increased from  $-1$  (other than the smoothing of the kinks/discontinuities), and when  $Lq_{0,2}$  is less than about  $\frac{\pi}{2}$  the force is always attractive.

The correspondence between  $\delta$ -spectra and parabolic spectra for positive  $\eta$  also holds for negative as well as complex  $\eta$ . If  $\eta = e^{i\theta}$ , there are kinks/discontinuities at  $Lq_{0,1,2} = n\pi \pm \frac{\theta}{2}$ , which smooth out as  $\eta$  is varied along the radius of the unit circle. Singular behavior can only occur when  $\eta$  is varied to 1, cf. Eqs. (4), (13), and (15). One can verify all this by evaluating Eqs. (2)-(3), (11)-(12), (14), (16) for any  $\eta$  in the unit disk, taking only the real part of  $P$  to get the desired acoustic Casimir force when  $\text{Im}[\eta] \neq 0$ .

## References

- [1] H. B. G. Casimir, “*On the attraction between two perfectly conducting plates,*” Proc. K. Ned. Akad. Wet. 51, 793 (1948).
- [2] A. Larraza, C. D. Holmes, R. T. Susbilla, and B. Denardo, “*The force between two parallel rigid plates due to the radiation pressure of broadband noise: An acoustic Casimir effect,*” J. Acoust. Soc. Am. 103, 2267 (1998).
- [3] J. Bárcenas, L. Reyes, and R. Esquivel-Sirvent, “*Acoustic Casimir pressure for arbitrary media,*” J. Acoust. Soc. Am. 116, 717 (2004).
- [4] A. A. Lee, D. Vella, and J. S. Wettlaufer, “*Fluctuation spectra and force generation in nonequilibrium systems,*” Proc. Nat. Acad. Sci. 114, 9255 (2017).
- [5] T. Emig, A. Hanke, R. Golestanian, and M. Kardar, “*Normal and lateral Casimir forces between deformed plates,*” Phys. Rev. A 67, 022114 (2003).
- [6]  $E_m(z)$  is given by the Wolfram Language function `ExpIntegrate[m, z]`. E. W. Weisstein, “*E<sub>n</sub>-Function,*” MathWorld—A Wolfram Web Resource. <<https://mathworld.wolfram.com/En-Function.html>>
- [7] A. Hanke, “*Non-Equilibrium Casimir Force between Vibrating Plates,*” PLoS ONE 8, e53228 (2013).